

1. Introduction

It is important to describe the long-term mean flow in the deep ocean to understand the ocean general circulation, which plays an important role in the climate system. Many oceanographers have deployed long-term mooring systems at key places in the deep to bottom layers to measure the deep-ocean circulation. Current meters used in deep-ocean moorings must be very sensitive since the deep flow is generally weak. The RCM8 current meter manufactured by Aanderaa Instruments (*Aanderaa Instruments*, Attleboro, MA, USA; *Aanderaa Instruments*, 1987), with a mechanical rotor and vane, has long been the most widely used current meter. However, the RCM8 has problems related to its mechanical workings. For example, its response to a weak flow is slow, and a flow of 1.1 cm s^{-1} or less cannot be measured.

Many oceanographers have recently begun to use new current meter designs, such as acoustic Doppler backscatter-based current meters, those based on the measurement and comparison of direct-path acoustic phase shifts along multiple paths, and electromagnetic current meters. It is necessary to know the characteristics of each current meter in observations where current meters based on different principles of measurement principles must be used. This requires a comparison of observations obtained during field tests. Since mooring observations are expensive and require substantial effort, there is not much information for inter-calibrating current meters with different measurement principles. The limited literature includes *Frye* (2002) and *Frye et al.* (2004), who reported the results of a comparison of several current meters in newly developed mooring systems. Their research revealed unexpected differences in measured speed and direction among those current meters. A similar but more thorough analysis of the same data appeared in *Hogg and Frye* (2007), where they added the results from the comparison between the appropriate velocity component of each instrument and the rate of change of pressure when they were lowered from a ship. They stressed that the RCM11 (Aanderaa; acoustic Doppler backscatter) records lower current speeds than those indicated by their referenced instruments, the VACM/VMCM (the vector averaging current meter/vector measuring current meter), although its direction records are of high quality (*Minken*, 2000). *Gilboy et al.* (2000) compared the results obtained by three systems, the three-dimensional acoustic current meter (3D-ACM; Falmouth Scientific, Inc., Cataumet, MA, USA; *Falmouth Scientific Inc.*, 1999), VMCM, and acoustic Doppler current profiler (ADCP) and found that they are in agreement within statistical error except for a 20° – 30° directional discrepancy attributed to the 3D-ACM. In addition, a European group in the French Research Institute for Exploitation of the Sea (IFREMER) recently collected several global datasets of parallel observations with different current meters (including part of our

data) and completed a comparative study that focused on the differences between mechanical instruments (mainly the RCM8) and newer ones (*A. Tengberg*, personal communication). They also found fairly large differences in the current direction indicated, particularly at low current speeds. The same group also conducted a tow-tank test for various current meters in IFREMER (*A. Tengberg*, unpublished data), which indicated that errors in current speed and direction are generally substantial at low current speeds, not only with mechanical instruments but also with other newer designs.

We have had a series of mooring systems deployed in the western equatorial Pacific since 1998 to observe deep currents below 2000 m. The purpose and background of this series of deep-mooring observations are described in section 2. In 2000 during this series of observations, we introduced a new type of current meter in this series of mooring observations, the 3D-ACM, in addition to the RCM8 already in use. We needed to compare the results of the two current meters to assess the accuracy of the observations. We also introduced two additional current meters, the RCM11 and the Compact-EM (EM; Alec Electronics, Kobe, Japan), to further clarify the characteristics of our two primary current meters, the RCM8 and 3D-ACM.

We made parallel observations using either two or four different current meters on five mooring systems to compare the results. Four different current meters were deployed on the first mooring of the five (Oct 2000 to Nov 2001) for a comparison at about 2500 m. Only two current meters, the RCM8 and 3D-ACM, were deployed at 2750 m on each of the remaining four moorings, two starting in July 2003 and two more in February 2004.

We compared the data to clarify the characteristics of each current meter type. Section 2 briefly explains the nominal features of the four kinds of current meters and the data-processing procedures. This section also includes a description of the purpose and background of the series of deep-mooring observations. The results are described in section 3. Finally, section 4 summarizes our conclusions and provides a discussion.

2. Data and observations

Figure 1 depicts the mooring locations and the design of the mooring system for the first set of

observations. Summary information for all three sets of observations is presented in Table 1. The first mooring was at 3°00.82'S, 162°12.40'E, with a bottom depth of 3261 m and an observation depth of 2500 m. The duration of observations was about one year, from 19 October 2000 to 7 November 2001. The current meters deployed were the RCM8, RCM11, 3D-ACM, and EM. The specifications of each current meter and observation setting are presented in Table 2. Three current meters, the RCM8, 3D-ACM, and EM were connected one over the other, separated by 10 m of rope. The RCM11 was connected with a stainless steel shackle directly below the EM (Figure 1b). The record length for the comparison was set to a uniform 353 days to match the duration of data collection of the 3D-ACM, which had battery trouble. The data for comparison (raw data) were obtained every two hours, and that data set was subsampled once a day at 1200 JST after smoothing twice using a 25-h running mean (filtered data). A recorded value of 1.1 cm s⁻¹ was treated as 0.0 cm s⁻¹ because the RCM8 cannot measure flow slower than 1.1 cm s⁻¹, recording it as 1.1 cm s⁻¹.

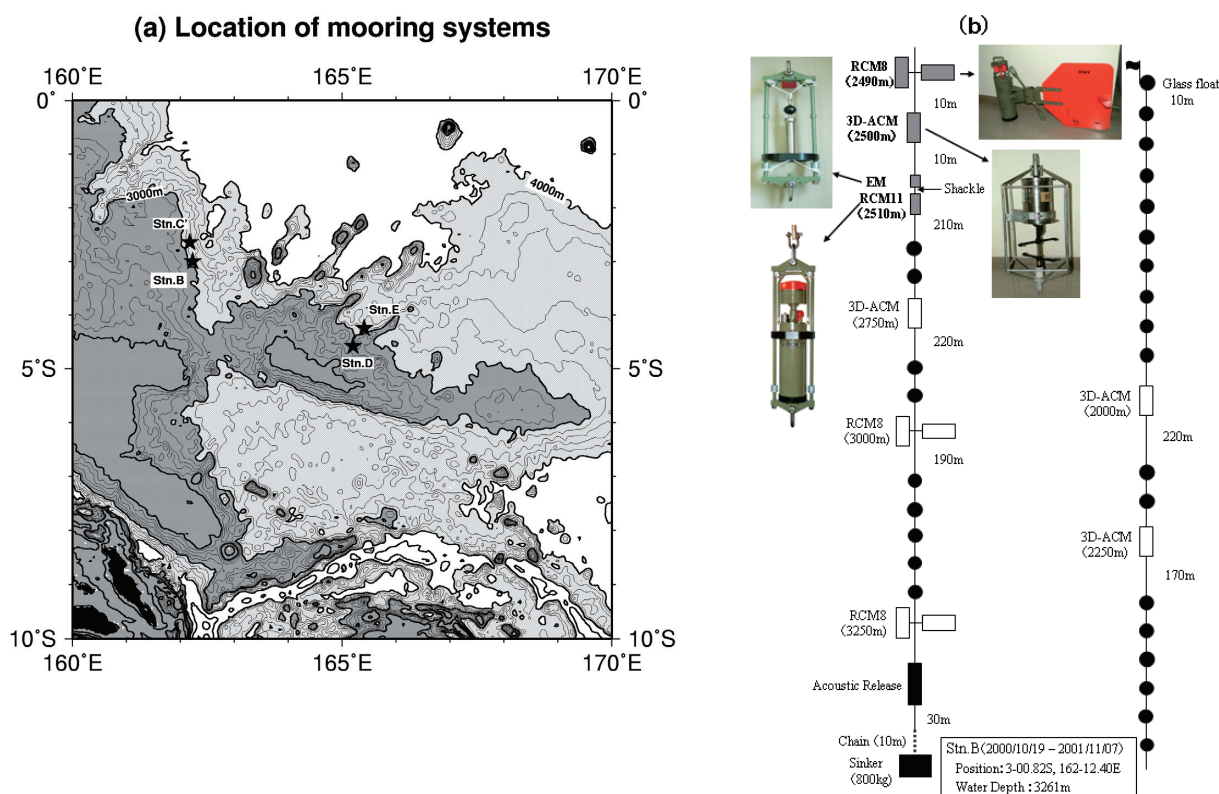


Figure 1. (a) Location of mooring sites. The light (dark) shading indicates regions with a depth between 3000 and 4000 m (between 0 and 3000 m). Isobaths are indicated between 2000 and 4000 m with a 200-m interval based on ETOPO2 (2-minute Gridded Global Relief Data, NGDC, NOAA, USA). (b) Design of the mooring at Stn. B for the first set of observations.

Each mooring in the second and third sets of observations included a 3D-ACM and an RCM8 current meter separated by 10 m at a depth of about 2750 m. The respective sampling intervals for the 3D-ACM and RCM8 meters were 20 minutes and 1 h. The original 3D-ACM data were sampled every hour at the same time as the RCM8 data point for comparison (raw data). The data were filtered and subsampled using the same procedure as described for the first set of observations. The duration of data collection was only 65 days for the RCM8 at Stn. E (Table 1). The duration of the data record used for comparison at each mooring was set to the shortest period of recorded observations.

Table 1. Locations of the mooring systems, mooring configurations, and numbers of data points for raw and filtered data.

	Depth	Sampling interval	Sampling mode	Record length (raw data: hours)	Record length (Filtered data: days)
(a) First Observation					
Stn.B (3-00.82S, 162-12.40E : Water depth 3261 m) 2000/10/19 - 2001/11/7					
RCM8	2490 m	2 hour	Averaging	4606	381
3D-ACM	2500 m	1 hour	Burst	4261	353
EM	2510 m	2 hour	Burst	4606	381
RCM11	2510 m	2 hour	Burst	4606	381
(b) Second Observation					
Stn.D (4-35.01S, 165-12.00E : Water depth 2730 m) 2003/07/23 - 2004/07/14					
3D-ACM	2670 m	20 min.	Burst	8564	354
RCM8	2680 m	1 hour	Averaging	8564	354
Stn.E (4-14.90S, 165-24.60E : Water depth 3300m) 2003/07/23 - 2004/07/14					
3D-ACM	2750 m	20 min.	Burst	8563	354
RCM8	2760 m	1 hour	Averaging	1600	65
(c) Third Observation					
Stn.B (3-00.05S, 162-13.63E : Water depth 3349 m) 2004/02/14 - 2005/02/12					
3D-ACM	2750 m	20 min.	Burst	8730	361
RCM8	2760m	1 hour	Averaging	8730	361
Stn.C' (2-39.01S, 162-10.28E : Water depth 3718 m) 2004/02/13 - 2005/02/12					
3D-ACM	750 m	20 min.	Burst	8757	362
RCM8	2760 m	1 hour	Averaging	8757	362

The present series of deep-mooring observations are designed to answer a specific question concerning deep-water circulation in the Pacific Ocean. Historical hydrographic and mooring data indicates that Lower Circumpolar Deep Water (LCDW) flows northward, crossing the equator, and enters the North Pacific (*Johnson and Toole*, 1993; *Roemmich et al.*, 1996; *Kawabe et al.*, 2003; *Siedler et al.*, 2004). It is then vertically mixed with upper-layer waters to form North Pacific Deep Water (NPDW) (*Mantyla*, 1975). The NPDW, which fills the deep layer (2000 to 3000 m) over the North Pacific, travels south, crossing the equator again back into the South Pacific (*Mantyla*, 1975; *Fiadeiro*, 1980). *Ishizaki* (1994) presented this circulation image using a simulation based on a Pacific Ocean model. The results of this model indicate that NPDW crosses the equator in the Melanesia Basin, northeast of Papua, New Guinea, but this is not evident from field observations. We have had mooring systems deployed near the equator since 1998 to clarify the location where NPDW crosses the equator. The results from these deployments will be presented in forthcoming papers.

Table 2. Specifications of the four current meters.

	RCM8	3D-ACM	EM	RCM11
	AANDERAA Instruments (NORWAY)	Falmouth Scientific, Inc. (U.S.A)	ALEC Electronics (JAPAN)	AANDERAA Instruments (NORWAY)
(a) Current speed				
Type	Rotor	Acoustic (Phase shift)	2-axis electro-magnetic	Acoustic (Doppler)
Range (cm s ⁻¹)	2 to 295	0 to 300	0 to ±500	0 to 300
Accuracy	±1 cm s ⁻¹ or ±2%	1 cm s ⁻¹ or ±2%	±1 cm s ⁻¹ or ±2%	±0.15 cm s ⁻¹ or ±1%
Resolution (cm s ⁻¹)	-	0.01	0.02	0.3
(b) Direction				
Type	Magnetic compass	3-axis fluxgate	Hall-element compass	Hall-element compass
Range (degree)	0 to 360	0 to 360	0 to 360	0 to 360
Accuracy (degree)	±5 (5 to 100 cm s ⁻¹) ±7.5 (2.5 to 5 and 100 to 200 cm s ⁻¹)	±2	±2	±5 (0 to 15 degree tilt) ±7 (15 to 35 degree tilt)
Resolution (degree)	0.35	0.01	0.01	0.35

3. Results

Stick diagrams of the filtered data and their time-averaged vectors are shown in Figures 2 and 3, respectively. The values of the time-averaged vector components from the raw data and the filtered data are given in Table 3. Direction is clockwise degree from true north ($^{\circ}$ T). The time-averaged values for the raw data and those for the filtered data are almost the same; the difference is less than 9% in speed and less than 1° in direction. We hereafter primarily discuss the filtered data. The temporal flow patterns recorded by the four current meters in the first set of observations show a similar tendency over the entire period, but the current speeds recorded by the RCM8 and RCM11 meters were lower than those of the other two (Figure 2a). This same tendency is also reflected in the time-averaged flow vectors (Figure 3a), in which the current speed and direction from the 3D-ACM and EM appear to be almost the same and the current speeds from the RCM8 and RCM11 are lower.

The current speeds recorded by the 3D-ACM were greater than those of RCM8 in all of the moorings except at Stn. B during the third set of observations. It is noteworthy that the time-averaged current direction of the RCM8 is always rotated clockwise from that of the 3D-ACM (Figure 3). The directional difference ranged from 10.6° at Stn. B in the first set of observations to 42.2° at Stn. B during the third set of observation. Following subsections present a more detailed examination of these different results.

3.1 First set of observations

The filtered data from the first set of observations were used to compare the current speed and direction recorded by the 4 types of meters by pairs (Figure 4). The current speeds indicated by the RCM8 were lower than those of each of the other three with an almost linear relationship. The RCM8 current direction was rotated clockwise relative to the others over the entire direction range except in a relatively narrow range between 330° and 120° , from north-northwest to east-southeast, in which the flow vector of the RCM8 was rotated slightly counterclockwise from those of the other meters (Figures 4a, b, and c). The EM current speeds showed a nonlinear relationship with those of the 3D-ACM and RCM11, suggesting a slower increase in the difference between recorded velocities for currents exceeding 10 cm s^{-1} (Figures 4d and f).

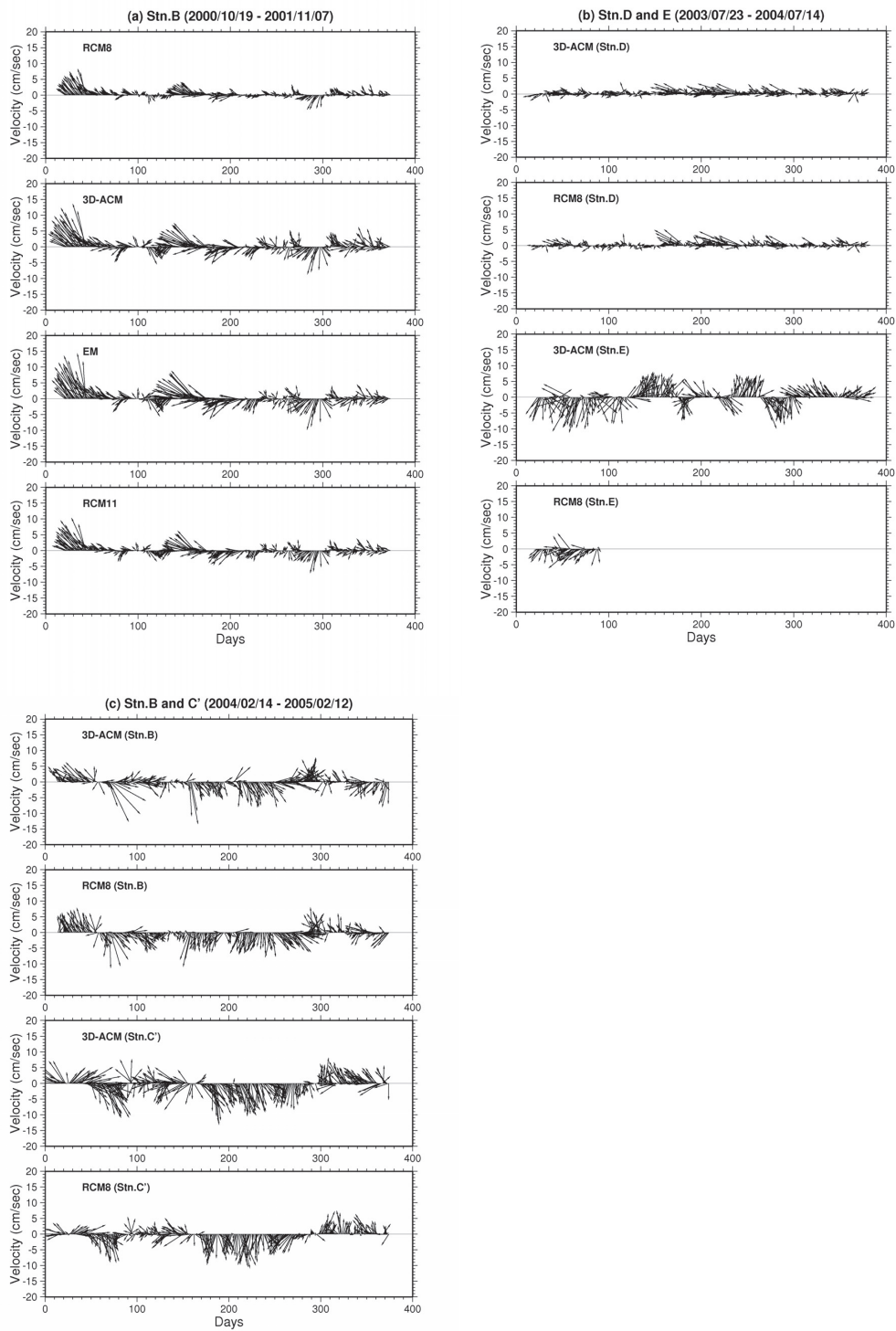
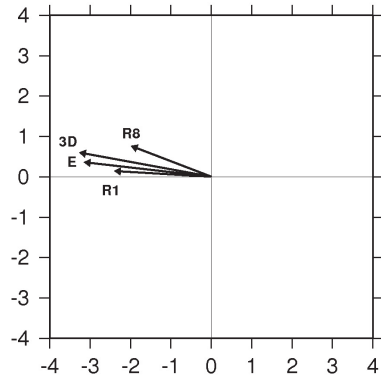
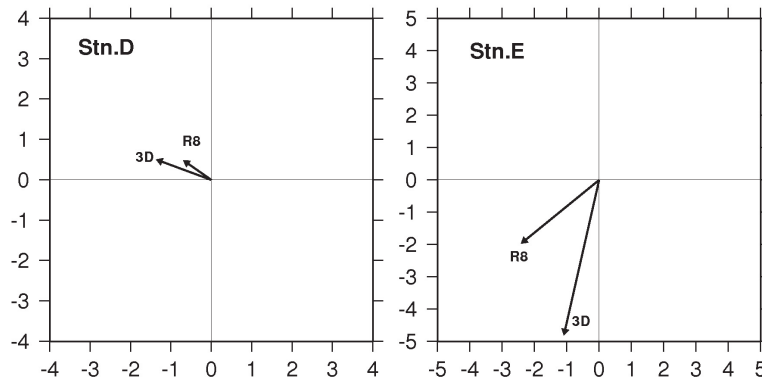


Figure 2. Stick diagrams of the filtered data for all current meters. (a) The first set of observations (Stn. B), (b) the second set of observations (Stns. D and E), and (c) the third set of observations (Stns B and C'). The abscissa is the day number, beginning on the first day of the first month in which data were recorded.

(a) Stn.B (Mean velocity vector)



(b) Stn.D and E (Mean velocity vector)



(c) Stn.B and C' (Mean velocity vector)

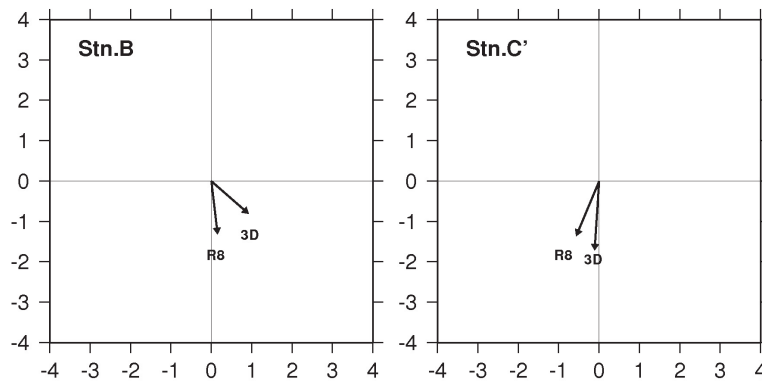


Figure 3. Time-averaged velocity vectors for all current meters. (a) The first set of observations, at Stn. B; (b) second set of observations, at Stns. D (left) and E (right); and (c) third set of observations, at Stns. B (left) and C' (right). Velocities are in cm s^{-1} . R8: RCM8; 3D: 3D-ACM; E: EM; R1: RCM11.

Table 3. Time-averaged flow statistics from raw and filtered data. The east–west and south–north components are given by u and v . Direction is clockwise degree from true north ($^{\circ}$ T).

	Raw data				Filtered data			
	u (cm s^{-1})	v	Direction (degree)	Speed (cm s^{-1})	u (cm s^{-1})	v	Direction (degree)	Speed (cm s^{-1})
(a) First observation								
Stn.B (2000/10/19 - 2001/11/7)								
RCM8	-2.16	0.83	291.0	2.31	-1.99	0.76	291.0	2.13
3D-ACM	-3.55	0.66	280.5	3.61	-3.28	-0.60	280.4	3.33
EM	-3.42	0.39	276.6	3.44	-3.16	0.35	276.5	3.18
RCM11	-2.60	0.16	273.4	2.61	-2.40	0.14	273.3	2.41
(b) Second observation								
Stn.D (2003/07/23 - 2004/07/14)								
3D-ACM	-1.36	0.50	290.4	1.45	-1.36	0.51	290.3	1.46
RCM8	-0.69	0.49	305.4	0.85	-0.70	0.49	304.9	0.85
Stn.E (2003/07/23 - 2004/07/14)								
3D-ACM	-0.20	-0.89	193.2	0.91	-0.20	-0.88	192.8	0.91
RCM8	-0.44	-0.37	230.8	0.58	-0.44	-0.36	230.8	0.57
(c) Third observation								
Stn.B (2004/02/14 - 2005/02/12)								
3D-ACM	0.92	-0.80	131.1	1.22	0.92	-0.81	131.1	1.23
RCM8	0.15	-1.31	173.5	1.32	0.15	-1.32	173.3	1.33
Stn.C' (2004/02/13 - 2005/02/12)								
3D-ACM	-0.14	-1.70	184.8	1.70	-0.11	-1.72	183.8	1.72
RCM8	-0.59	-1.36	203.6	1.48	-0.57	-1.36	202.7	1.47

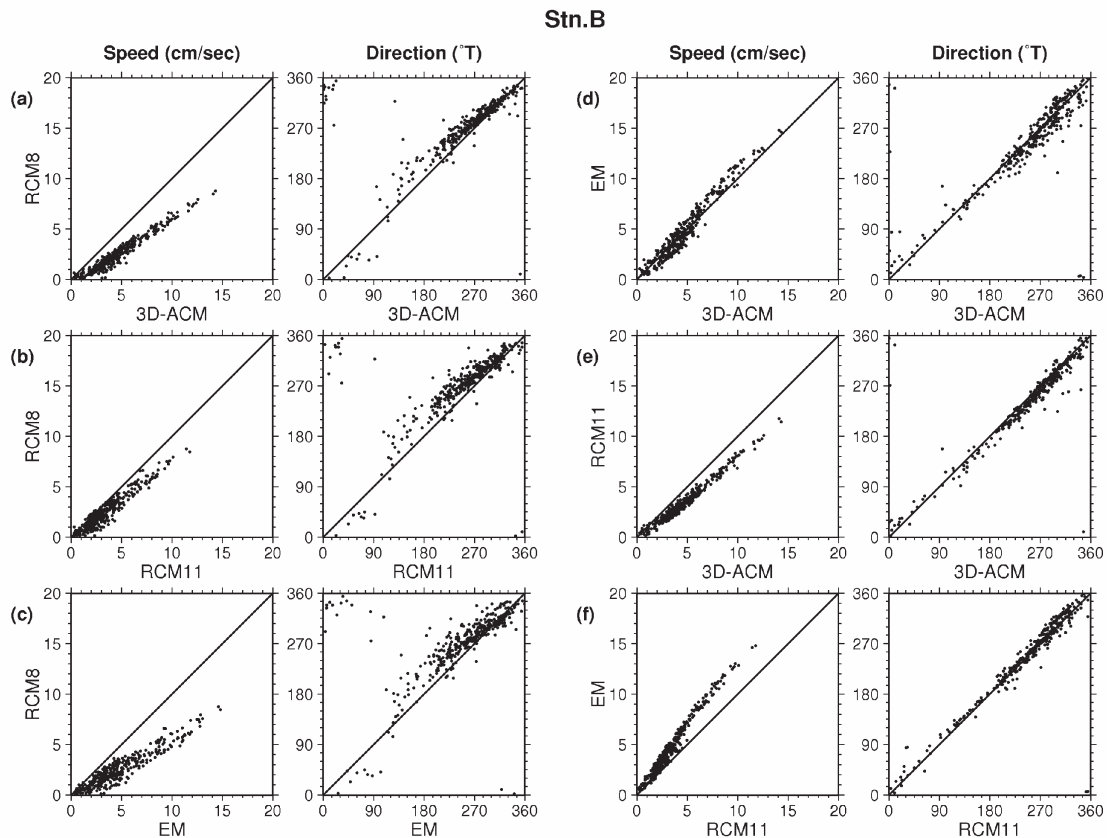


Figure 4. Scatter plots of current speed and direction, using filtered data, for each pair of the four current meters used in the first set of observations. (a) RCM8 vs. 3D-ACM, (b) RCM8 vs. RCM11, (c) RCM8 vs. EM, (d) EM vs. 3D-ACM, (e) RCM11 vs. 3D-ACM, and (f) EM vs. RCM11. Direction is clockwise degree from true north ($^{\circ}$ T).

We also performed a time-series comparison of current speed and directional difference for each pair of current meters, based on the filtered data (Figure 5). Significant differences in direction, which appear as spikes, generally corresponded to weak flows. We first compared the RCM8 with the other three current meters (Figures 5a, b, and c). The current speed of the RCM8 was always less than that of each of the other three, as expected (see Figures 2 and 3). The directional difference between the RCM8 and each of the other three meters exhibited similar temporal patterns, with the difference being generally positive, also as expected (see Figure 3). Note that the magnitude of the difference in direction appeared to be inversely correlated with the current speed, except for the spike-like variations; the higher the current speed, the smaller the difference in direction. This inverse relationship is evident in the long-term variation over the first half of the observation period, or about 120 days. This relationship was also evident in the short-term variations with a period of about 10 days.

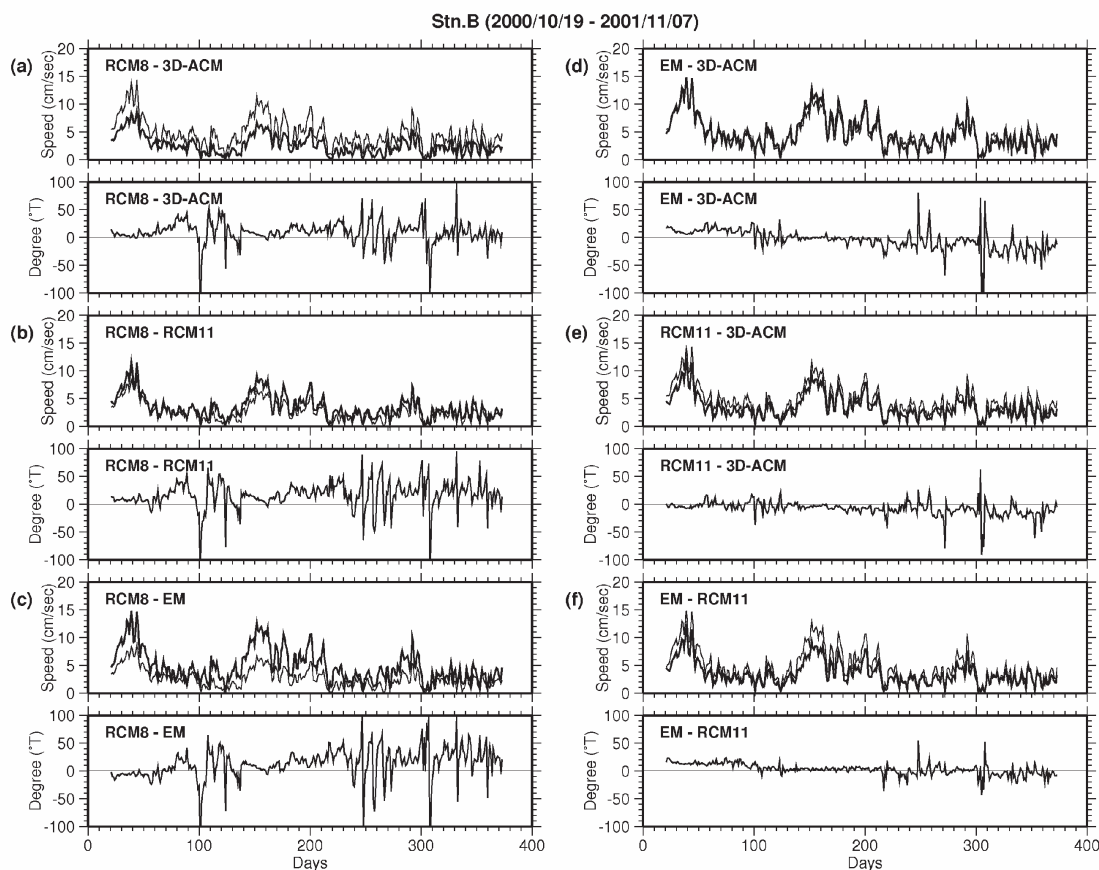


Figure 5. Time-series of current speed and the difference in direction for each pair of current meters used in the first set of observations. The order of the pairs is the same as in Figure 4. Thick lines in the panels for speed denote (a) RCM8, (b) RCM11, (c) EM, (d) EM, (e) RCM11, and (f) RCM11. The directional difference is defined as the direction of the first listed current meter minus that of the second in each pair. The abscissa is the day number, beginning on the first day of the first month in which data were recorded.

In the three remaining comparisons (Figures 5d, e, and f), the temporal patterns in the current speed of the 3D-ACM and EM were almost the same; the current speed of RCM11 was somewhat lower than those of both the 3D-ACM and EM (see Figures 2 and 3). The differences in direction were generally small compared to those relative to the RCM8. However, there is a trend with a descending slope in the paired comparison between the EM and 3D-ACM and the RCM11 and 3D-ACM (Figures 5d and e). By the end of the observation period, these differences had reached approximately -30° and -15° , respectively. In addition, the comparison between the EM and RCM11 demonstrated discontinuous changes in the directional difference around days 100, 225, and 300, at about 10° each (Figure 5f). These changes appear

to be related to low current speeds. The difference in direction was stable at other times. These discontinuous changes can also be seen in the comparison between the EM and 3D-ACM, superposed on the descending trend (Figure 5d). Thus, we deduce that the temporal trend in the difference in direction in this comparison came from the 3D-ACM and that the discontinuous changes originated from the EM current meter.

For each pair of current meter types, we compared the directional difference with the current speed of one current meter of the pair, using the filtered data (Figure 6). It is noteworthy that in comparisons between the RCM8 and the other three meters, there is an inverse relationship between the magnitude of difference in current direction and the current speed of the RCM8 over the entire current range (Figures 6a, b, and c). The directional differences were all positive values for higher current speeds, or at least greater than that at the highest current speeds. The directional difference was zero or even negative at the highest current speeds; however, the difference in direction of the time-averaged flows was positive (Figure 3a) because of the inverse correlation between current speed and the directional difference.

In the comparisons between the EM and 3D-ACM and the EM and RCM11, two clusters of directional differences, separated by about 10° , can be clearly seen at current speeds greater than 5 cm s^{-1} (Figures 6d and f). These two clusters correspond to the periods before and after the discontinuous change in the directional difference around day 100 (Figures 5d and f). The current speed did not exceed 5 cm s^{-1} for the period after day 300; thus, the corresponding points do not form a clear peak at high current speed but rather appear as a clump with negative values (Figures 6d and f). The paired comparison between the RCM11 and 3D-ACM also displayed increased scatter for current speeds between 2 and 7 cm s^{-1} , and this seems to come from the temporal trend in the direction record of the 3D-ACM as was deduced before (Figure 5d and e). Unlike the comparisons that included the RCM8, we could not identify any definite relationship between current speed and the difference in direction in the comparisons that did not include the RCM8.

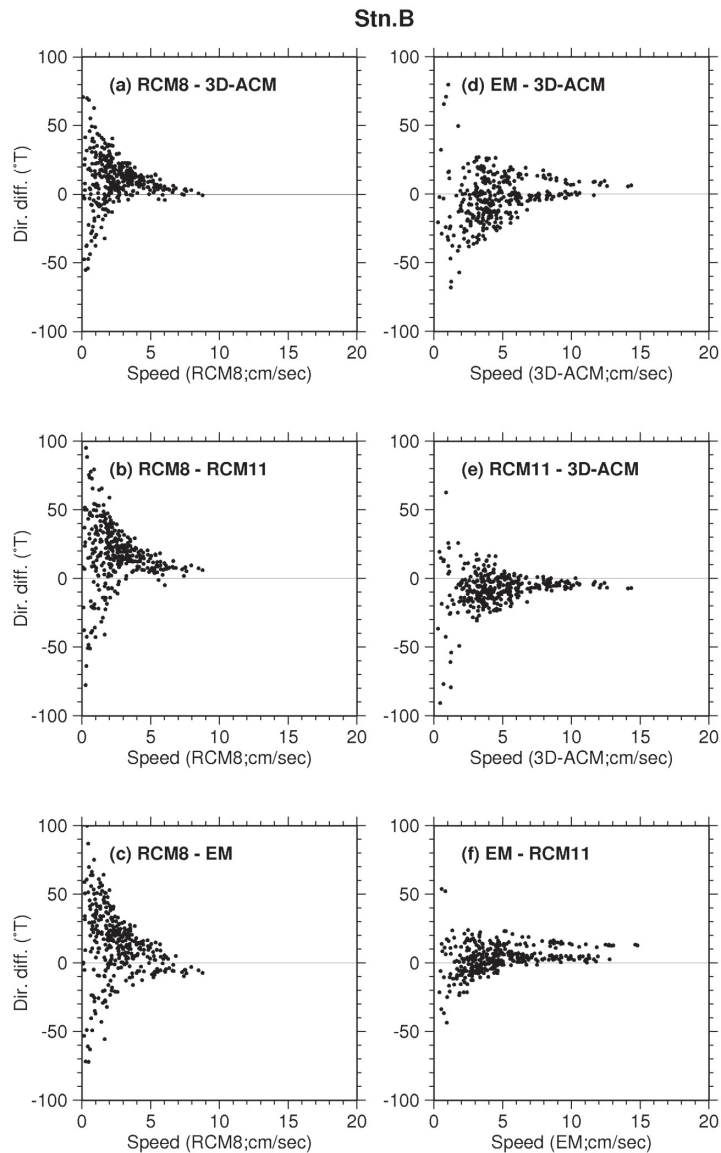


Figure 6. Scatter plots of the difference in direction versus the speed recorded by one current meter of each pair.

The order of the pairs is the same as in Figure 4.

3.2 Second and third sets of observations

The second and third sets of observations involved a comparison only between the RCM8 and 3D-ACM. The scatter diagrams for speed in Figure 7 reveals various deviations from the linear relationship. The only obvious linear relationship was at Stn. E, but the duration of data collection there was very short (65 days). At Stn. D, the speed measured by the 3D-ACM was generally greater than that measured by the

RCM8; at the highest current velocities ($>8 \text{ cm s}^{-1}$), there was an almost linear relationship with a slope of one. This general relationship was reversed at Stn. B, with the speed measured by the 3D-ACM less than that of the RCM8 for currents weaker than 7 cm s^{-1} . Station B was unique in that the time-averaged flow speed from the RCM8 was greater than that of the 3D-ACM (see Figure 3c). At station C¹ there were two different patterns evident at speeds greater than 5 cm s^{-1} that can be deduced from the time series for current speed for this station (Figure 8d), in which the speed measured by the 3D-ACM was generally greater than that of the RCM8 over the entire observation period, except for between days 200 and 260, when the two curves almost coincided. The scatter in the directional data indicates a linear relationship with a consistent difference over the entire range of observations for all stations except Stn. D, where most of the points fall near the line indicating equality between the two meters, with some scattered points (Figure 7a). Some points just below the central declined line for Stn. C' (Figure 7d) came from the initial 15-day period (Figure 8d), when the sign of the directional difference was reversed.

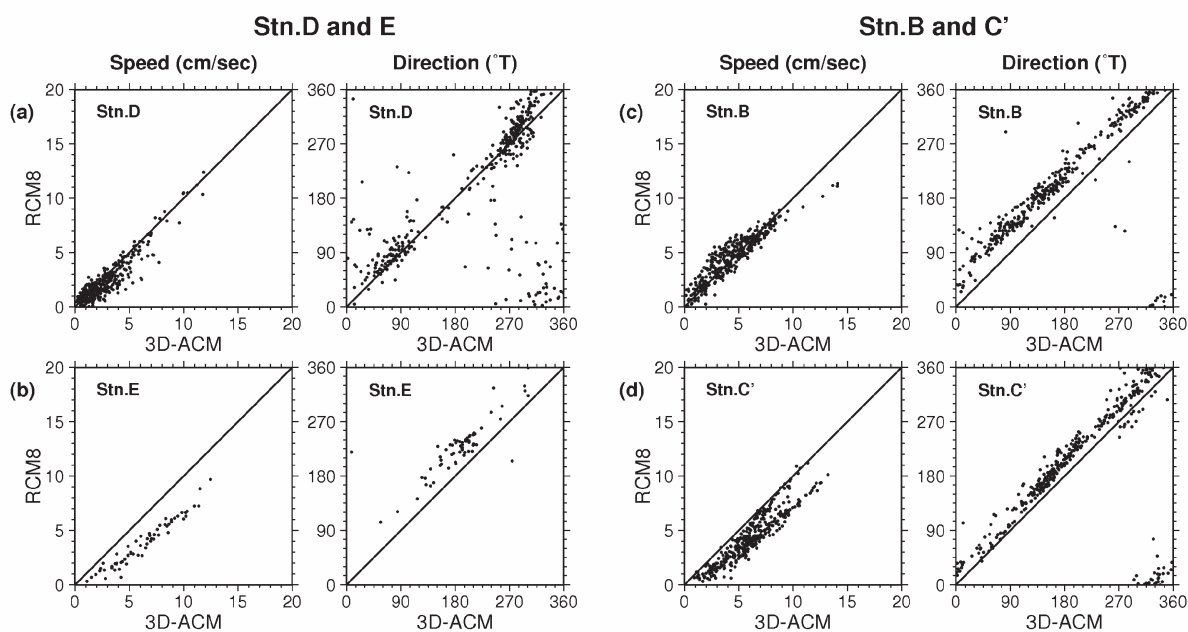


Figure 7. Scatter plots of current speed and direction for the filtered data from the second and third sets of observations. (a) Stn. D and (b) Stn. E from the second set of observations and (c) Stn. B and (d) Stn. C' from the third set.

¹ We made a mooring observation at station C near station C' but as different station in the same period as the first set of observation mentioned in this report. Therefore, we identify the location in the third sets of observation C'.

During the second observation period, at Stn. D, the current speed was relatively low and the difference in current direction between the two meters exhibited many spike-like variations without any clear, steady positive bias (Figure 8a). In contrast, the other three comparisons showed high, steady positive values for the directional difference between the two meters, with a short-term shift over the first 50 days at Stn. C' during the third observational period (Figures 8b, c, and d). There is a clear, inverse relationship between current speed and the difference in direction for all comparisons except at Stn. D, where the points scatter almost evenly around the current speed peak at about $+5^\circ$ (Figure 9). The difference in direction at the highest current speeds, around 10 cm s^{-1} , was a relatively high positive value for the three cases with a clear inverse relationship, that is, about $+30^\circ$, $+25^\circ$, and $+15^\circ$ for Stns. E, B, and C', respectively (Figure 9). The actual directional differences for the time-averaged flows listed in Table 3 for these three stations were $+38.0^\circ$, $+42.2^\circ$, and $+18.9^\circ$, respectively, which are greater than those at the highest current speeds, as was also noted for the comparisons between the RCM8 and other meters during the first set of observations (Table 3 and Figures 6a, b, and c). In addition, the difference in direction for the time-averaged flow for Stn. D, $+14.6^\circ$, was greater than that for the peak current flow, $+5^\circ$. A comparison of the difference in current direction and current speed as measured by the 3D-ACM, using raw data, shows that the difference in direction was stable for speeds greater than 10 cm s^{-1} (Figure 10).

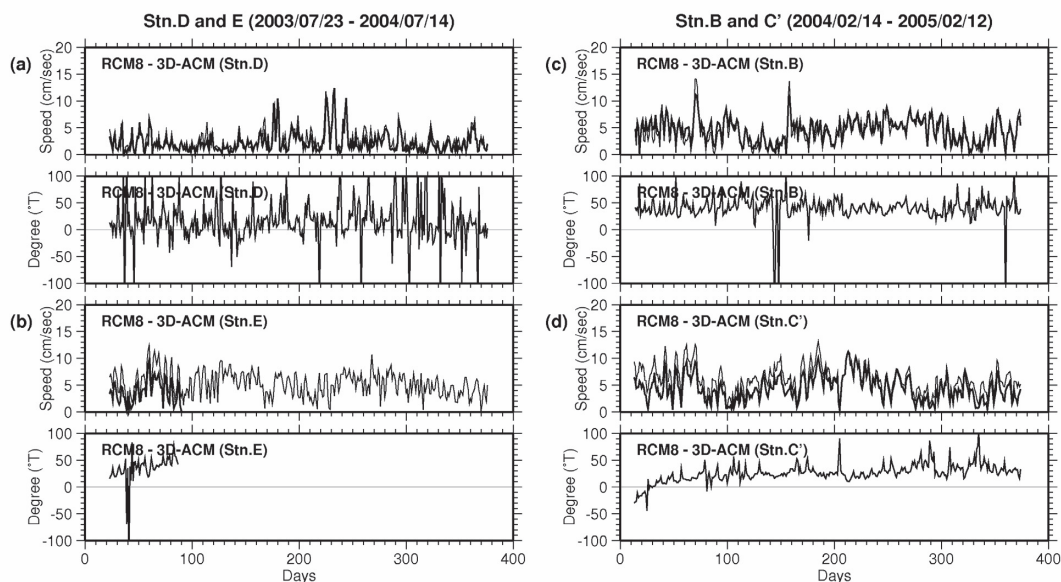


Figure 8. Time-series of current speed and the difference in direction for each pair of current meters during the second and third sets of observations. Thick lines in the panels for speed denote the RCM8, and thin lines, the 3D-ACM. The difference in direction is defined as the direction recorded by the RCM8 minus that recorded by the 3D-ACM. The abscissa is the day number, beginning on the first day of the first month in which data were recorded.

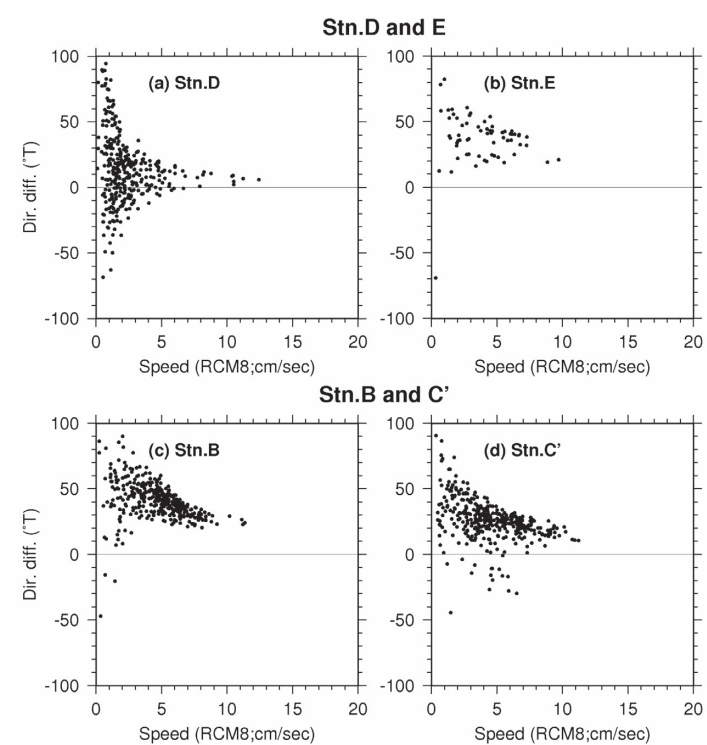


Figure 9. The difference in recorded current direction versus current speed recorded by the RCM8, using filtered data from the second and third sets of observations.

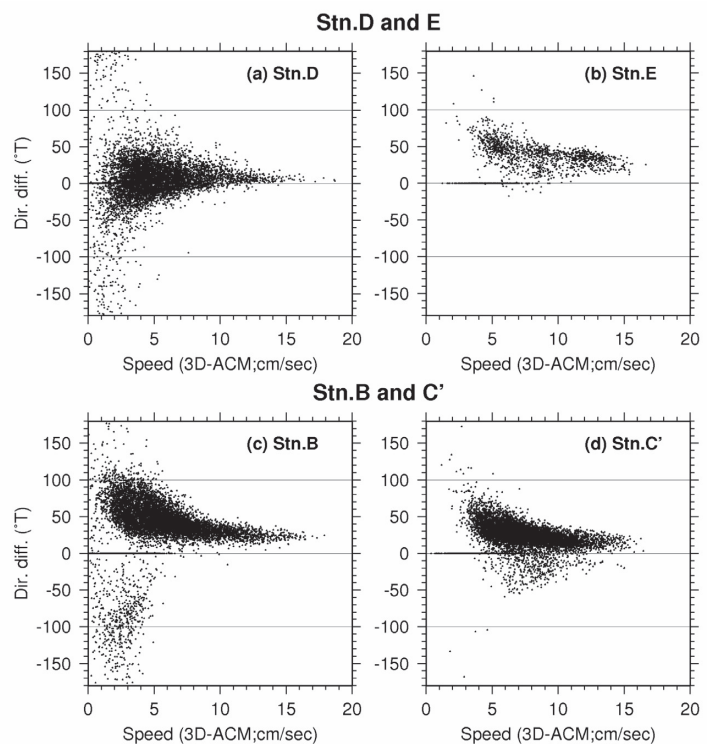


Figure 10. The difference in recorded current direction versus current speed recorded by the RCM8, using raw data from the second and third sets of observations. The abscissa is the current speed recorded by the 3D-ACM.

4. Summary and discussion

We compared current meter data obtained from deep-ocean moorings near the equator. There were three sets of observations, each with a duration of about one year. Four different models of current meter, the RCM8, RCM11, EM, and 3D-ACM, were set at approximately 2500 m at Stn. B for the first set of observations (Figure 1). For the second set of observations, moorings at Stns. D and E each had a 3D-ACM and an RCM8 meter at 2750 m. For the third set of observations, moorings at Stns. B and C' each had a 3D-ACM and an RCM8 meter at 2750 m. There were a total of four paired meter deployments in the 2nd and 3rd sets of observations. The primary results are as follows:

- (1) The results from the first set of observations indicate that the temporal flow patterns recorded by the four current meters exhibited a similar tendency over the whole observation period, but that the current speed indicated by the RCM8 was the lowest and that of the RCM11 was lower than the 3D-ACM and EM (Figure 2a). This tendency is also reflected in the time-averaged flow vectors (Figure 3a), in which the current speed and direction of the 3D-ACM and EM are almost the same and the current speeds of the RCM8 and RCM11 are lower.
- (2) The speed of the time-averaged flow of the RCM8 was generally lower than that of the 3D-ACM during the second and third observations, except at Stn. B during the third set of observations (Figures 3b and c).
- (3) The direction of the time-averaged flow of the RCM8 was always rotated substantially clockwise from those of the other current meters. The difference in direction from the 3D-ACM ranged from 10.6° at Stn. B during the first set of observations to 42.2° at Stn. B during the third (Figure 3 and Table 3).
- (4) A paired comparison of current speed data from the RCM8 with each of the other three current meters, using data from the first set of observations, indicates that the speed measured by the RCM8 was always lower than that of the other meters with an almost linear relationship (Figures 4a, b, and c; Figures 5a, b, and c). However, the speed measured by the RCM8 in the second and third sets of observations revealed various deviations from the linear relationship compared with the speed measured by the 3D-ACM (Figure 7a, c, and d). The deviations seem to be dependent upon the

particular conditions at each station.

- (5) The directional difference between the RCM8 and the other meters (the direction indicated by the RCM8 minus the direction indicated by each of the other meters) in the first set of observations was inversely correlated with the current speed; the lower the current speed, the greater the difference in direction (Figures 5a, b, and c; Figures 6a, b, and c). This difference in direction was asymmetrically positive and consistent with the relationship among the time-averaged current vectors (Figure 3a).
- (6) A similar inverse correlation between speed and directional difference can be seen in three of the four parallel observations by the RCM8 and 3D-ACM meters in the second and third sets of observations (Figures 9 and 10). The difference in direction in those observations for the highest speeds, around 10 cm s^{-1} , was consistently a high positive value ranging from 15° to 30° , not near zero. The current direction indicated by each RCM8 clearly had a consistent bias compared to that of the 3D-ACM. The directional difference between the time-averaged flows was greater than that for the highest current speeds because of the inverse relationship between the speed and the difference in direction.
- (7) A comparison among the three current meters other than the RCM8 during the first set of observations suggests that observational errors occurred, including a temporal trend in current direction in the 3D-ACM and discontinuous changes in current direction in the EM. The RCM11 appeared to be the most robust against errors in current direction. No definite relationship between speed and the difference in direction was noted in any paired comparison among these three current meters, as was observed in pairs that included the RCM8.

There are two factors to consider in the finding that the RCM8 generally had a positive bias in current direction relative to the other current meters. The first is the inverse relationship between current speed and directional difference from the other current meters (Figures 6, 9, and 10). This relationship clearly resulted from directional measurement errors by the RCM8 alone, since this correlation was not detected in any other comparison between pairs of the other current meters from the first set of observations. Although we do not have proof, we think one possible reason for the asymmetric distortion in current direction may be the existence of the shield for the rotor, which is located on the right side of the instrument, facing into the current. The inverse relationship was observed for current speeds below 10 cm s^{-1} both in the raw and filtered data; this means that the current speed threshold for correct functioning of

the RCM8 meter is around this value.

The second factor in the apparent directional bias of the RCM8 is the steady positive bias under strong currents in three of the comparisons in the second and third sets of observations (Figures 9 and 10). Only the RCM8 and 3D-ACM were compared in these observations, and thus we cannot directly determine from which current meter the errors originated solely from our observations. Following our field studies, we performed a laboratory calibration of the direction sensors of all RCM8 and 3D-ACM instruments used for the comparisons in the second and the third sets of observation and found errors on the order of $\pm 2^\circ$ against magnetic north in every instrument, but not errors as large as 15° – 30° as were observed in the deep ocean. Both *Gilboy et al. (2000)* and *Hogg and Frye (2007)* reported similar phenomena about the steady directional bias of the 3D-ACM. *Gilboy et al. (2000)*, while attempting to detect the current velocity at 72 m over a 110-day period, indicated that the direction measured by a 3D-ACM set at a depth of 72 m was up to 20° – 30° offset from those of a VMCA at 73 m and an ADCP set at 209 m. *Hogg and Frye (2007)* found a mean difference in direction of 15° – 20° over 54 days at 4000 m between their referenced VMCA/RCM11 and 3D-ACM against the reference direction. These values fall within the range of directional differences that we observed. Furthermore, the direction of offset is the same, that is, the current direction recorded by the 3D-ACM is rotated anticlockwise from those measured by the other instruments, as it was in our comparisons. Therefore, we deduce that the steady positive bias in direction for strong currents seen in three of the four comparisons in the second and third sets of observations (Figures 9 and 10) may come from the 3D-ACM. We believe that some of the laboratory calibration values installed into the instrument by the manufacturer (zero adjustment) may not have been correct for real ocean conditions of high pressure and low temperature.

Tow-tank tests indicate that the average direction errors not only for the RCM8 but also for the EM and 3D-ACM may be more than 10° , and often more than 40° , below current speeds of about 3 cm s^{-1} (Tengberg et al., unpublished data). However, the systematically asymmetric difference in direction of the RCM8 (Figures 6, 9, and 10) cannot be seen in the tow-tank tests. The duration of each tow-tank test was short, that is, several hours; thus, the average response of each current meter may differ from that during long-term moorings. These comparisons between meters may be complementary.

The RCM11 works by measuring the Doppler shift of back-scattered super-sonic sound signals first released in four directions; its measurement window is between 0.4 and 2.2 m from the sensor. This

differs from the EM and 3D-ACM, which measure the current near the sensor. The reduced current speed measured by the RCM11 may be a result of this spatial averaging. *Hogg and Frye (2007)* also stressed that the RCM11 speed values are generally less than those indicated by their referenced VACM/VMCM instruments, although its direction records are of high quality, observations consistent with our results.

We do not know the causes for observational errors such as the temporal trends and discontinuous changes in current direction that occurred in the 3D-ACM and EM. At Stn. C', where two distinct relationships between current meter speeds are evident (Figure 7d), the flow was predominantly southward during the period in which the speeds of the two current meters coincided. A certain range of current directions may generate errors in current speed measurements for either of the two current meters, but again we do not know the cause.

New current meter designs (acoustic or electromagnetic) provide superior performance and are easy to handle and care for, with increased battery capacity, substantial data-storage memory, shorter recording intervals if required, and simplified data processing. These new current meters are becoming more widely used. However, they also have specific characteristics and inherent errors that counteract their nominal accuracy, as reported in this report. Therefore, interaction and information exchange between manufacturers and field observers are important for improving instruments to obtain high accuracy data.